

Identification of Impending Interturn Faults in Random Wound Induction Motors Used in Adjustable Speed Drives

S.PONNUSWAMY RAJKUMAR, J.SUDESH JOHNY, A. EBENEZER JEYAKUMAR

Department of Electrical & Electronics Engineering

Sri Ramakrishna Engineering College

Coimbatore – 641 022

INDIA

hod-eee@srec.ac.in, john_plasma@srec.ac.in, ebeyjkumar@rediffmail.com

<http://www.srec.ac.in>

Abstract: - Diagnosis of stator current has been presented by several authors for identifying various bearing and rotor faults in an induction motor. However, there is very limited literature covering the effect of interturn faults on the stator current pattern. This is due to the reason that the effect of motor interturn insulation faults in the initial stages being not discernable and any changes in the capacitive current components are negligibly very small and of very high frequency content. This paper deals with a simple technique, utilizing the effect of the interturn fault in modifying the high frequency components of the applied pulse width modulated (PWM) voltage. Insulation Resistance (IR) and Polarization Index (PI) are two universally accepted diagnostic tests for insulation tests. The change in insulation strength between the turns affects the capacitive component of the stator line current. Resulting changes in wave shapes of applied voltage have been studied with respect to both the distance of interturn faults from line end and reduction in the insulation strength; and hence in the insulation resistance value. The studies have been made by computer simulation and validated by experiments. There is ample evidence that an impending and progressing interturn fault can be identified in Adjustable Speed Drives driven by frequency converters by studying line end coil voltage waveforms.

Key-Words: - Repetitive switching surges, Stator line current, PWM Voltage, Adjustable speed drives, Motor insulation, Interturn faults, High-frequency capacitive current components

1 Introduction

Induction motors have been the most preferred drives in the 20th century due to their robustness and easy availability. These motors are available from medium voltages to low voltages. While medium voltage motors use form wound coils, low voltage motors use either form wound or random wound coils. Interest in inter-coil and inter-turn voltage distribution started when medium voltage motors controlled by vacuum switches started failing due to surges generated by prestrikes and restrikes in the switch. Subsequently this problem was sorted out using better electrode materials.

Repetitive surges in Adjustable Speed Drives (ASD) have always been a concern right from 1920s [1]. Thyristors and Transistors formed the drives and the failures of motors were mostly due to either poor workmanship or material defect. However with the advent of fast switching devices like Insulated Gate Bipolar Transistors (IGBT) and

Metal Oxide Semiconductor Field Effect Transistors (MOSFET), there has been an increase in motor failures [2]. Such switching devices can generate repetitive voltage surges with very fast rise times of typically lower than 200ns. These fast rising voltages can cause a highly non-linear intercoil and interturn voltage distribution [3]. Switching over the existing motors as retrofits to be used with IGBT drives has compounded the problem [4, 5]. Failures of the motors have been attributed to insulation failure, bearing failure and rotor bar breakage failure. While bearing failures account for 50% of all motor failures, 22% of stator winding failures are ascribed to interturn failures [5]. Quite a few papers deal with the modification of stator current due to bearing faults, broken rotor bars; and suggest methods to identify such faults [6, 7].

With the advent of fast acting semiconductor switches, low voltage motors are

being used as inverter fed ASDs. The use of low voltage random wound motors as ASDs has made it difficult to identify an impending interturn fault [4,5]. This situation has necessitated the early identification of impending interturn faults to prevent unexpected breakdown of a critical drive.

Standards from IEC, IEEE and NEMA pertaining to rotating machines recommend test methods that mostly test only the quality of the insulation system and not the actual capability of the insulation system against repetitive surges. Hence, motors that pass such tests do not necessarily withstand the rigour of the operations [8]. Further, such standards have been able to recommend test procedures only for form-wound coils that have relatively very established manufacturing techniques [9].

Most important fact that “the ASD induced transient voltage pulse at the motor terminal penetrates into the winding via oscillatory and travelling wave modes; causing highest voltage stress between any two turns of winding anywhere from the first turns of the line end coil to the last turns of the coil group” was brought out only as late as 1997 by Melfi, et al. [2]. Effect of cables connecting the motors has also been studied [2]. These studies have proven that with the present-day low-loss cables, surges reach motor terminals un-attenuated [2]. IEEE-522, dealing with surge testing of motor coils is currently being revised but the changes are likely to be mainly clarifications [8].

2. Transient Voltage Distribution in Random-Wound Motors

For any surge, the motor winding presents itself like low-loss transmission line [10]. The stator core would provide the return path for the surge current since the active conductors are insulated. Surges travel un-attenuated in the winding and get reflected at coil junctions at stator and overhang portions of a coil. Capacitive coupling between the turns overrides inductive coupling between the turns at high frequencies [10].

2.1 Modelling of a typical random wound induction motor

For a surge impinging on the motor winding, the winding presents itself like transmission line. Most of the motors have very low winding resistance, exhibiting essentially a low loss transmission line. Inter-turn capacitive coupling to earth overrides any mutual inductive couplings. The core might be represented as a magnetic member with a very low

susceptance [10]. The stator core would provide the return path for the surge current since the active conductors are insulated. Further the stator windings are either connected in delta or in star with insulated neutral. Hence for most part of the winding, the surges would travel without attenuation and also get reflected at coil junction at stator and overhang portions of a coil. The deviation from uniform theoretical transmission line model values due to actual construction can aggravate the situation. Such a deviation is very pronounced in stator windings using random windings [3]. As far as the inter-turn coupling is concerned, for the high speeds of switching of IGBTs (typically <200ns), the inter-turn capacitive coupling can be safely assumed to be much greater than inter-turn mutual inductive coupling.

2.1.1 Winding Model (Fig.1)

The machine considered is a 3-phase, 50Hz, 415V, 1.5HP mush-wound, Δ -connected (Fig.2) induction motor with the following stator specifications:

Number of stator slots = 36; Number of coils per phase = 6; Conductors/slot = 50*

Stator bore diameter = 0.13m; Stator core length = 0.13m; Enamelled wire = 21 SWG

(*Actual design value is 104 conductors per slot. Since the investigation involves the first few turns of a coil, the motorette has been made with 50 conductors per slot. Hence, for simulation also the same data has been used).

For the physical parameters of the motor winding, calculations yield the following coil parameters:

Coil Resistance, $R_s=7.7 \text{ m}\Omega$; Inductance, $L=28\mu\text{H}$;

Earth Capacitance, $C=100\text{pF}$; Winding Insulation Resistance, $R_p= 1\text{G}\Omega$.

2.1.2 Line end coil modelling:

For the study of inter-turn voltages of the line end coil the following model has been considered:

The line end coil has been divided into three parts namely; i) distributed R,L,C parameters for the first three turns, ii) lumped parameters for the next 44 turns and iii) distributed parameters for the last three turns. This is based on the findings that the initial voltage distribution due to fast fronted surges in the line end coil is mostly decided by the first few turns [10, 11]. The line-end coil model has incorporated the effect of both the travelling waves and their scatter due to interturn and earth capacitance [11]. Further the variance of these capacitances in the slot and the overhang regions has also been taken into account. Any high frequency component of surge voltage would find a return path through the grounded stator frame. Each turn is allotted its respective R, L, C values based

upon its position as either in the slot region or the overhang region.

The inter-turn model assumes that in the slot region, six conductors placed on the periphery of the impulsed conductor can totally shield the conductor from all other conductors and from the core. Capacitance of the conductor subtended on the encircling conductors is used for slot region and a dielectric permittivity of 2.5 is chosen. However, due to the loose arrangement of the turns in the

overhang where the effect of air overrides the enamel insulation, air permittivity is used. All the unit distance values are converted into real values, using the overhang and slot lengths of the conductors. The coil is divided into cable side of the overhang, slot region and the overhang in the rear of the machine. The line end coil model is shown in Fig.3. Elaborate model of the first and last three turns of the line end coil is shown in Fig.4.

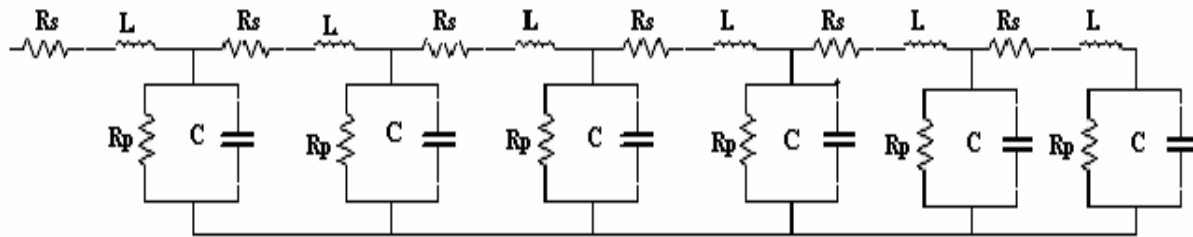


Fig.1 Winding Model

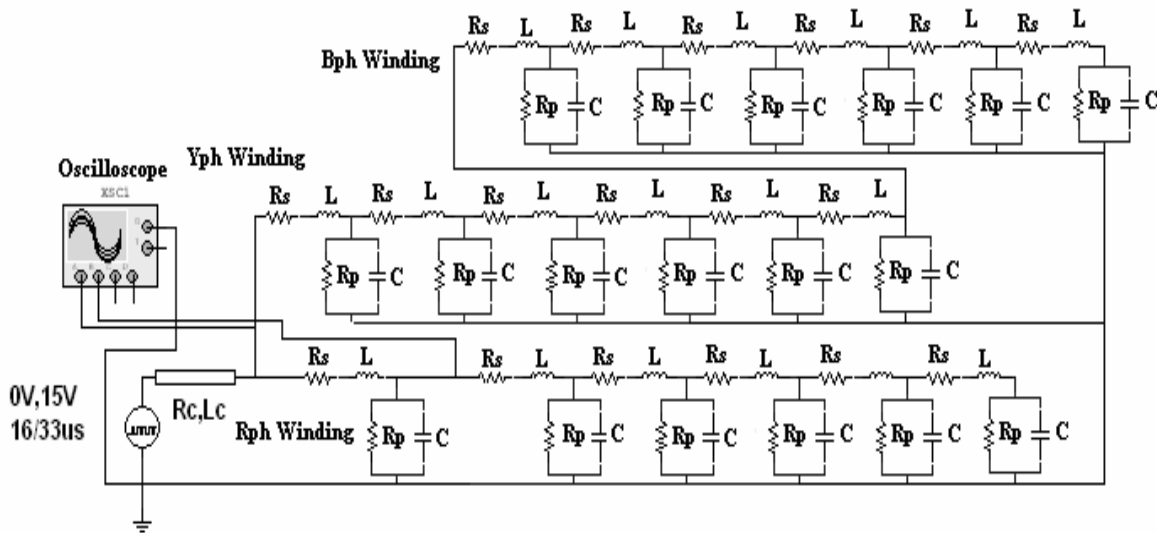


Fig.2 Winding in Δ connection with incomer cable

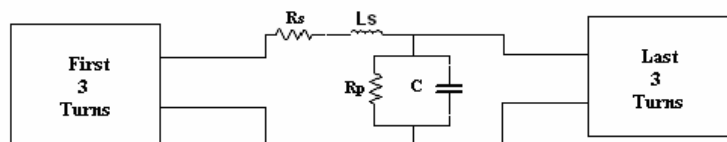


Fig.3 Line-end Coil Model

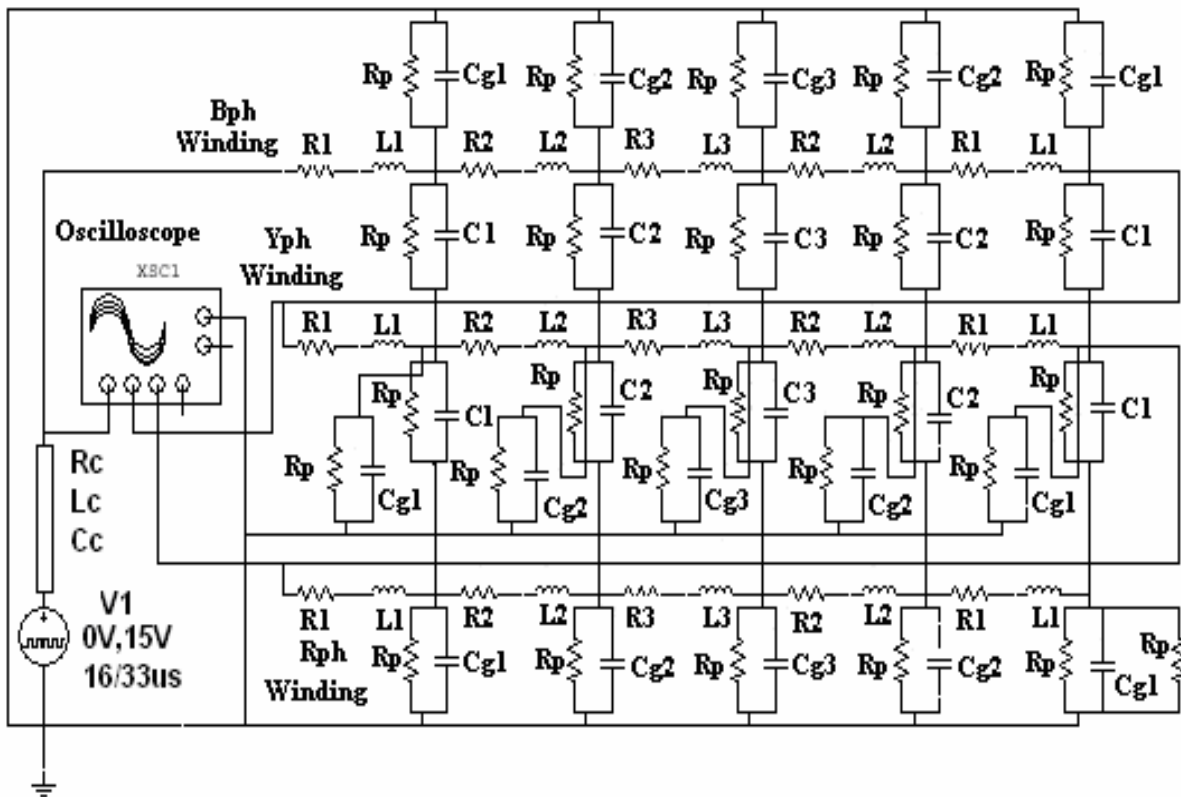


Fig.4 Line-end Coil Model with Distributed Parameters

Values of interturn parameters

Overhang parameters at line end side: $R_1 = 6.4\text{m}\Omega$; $L_1 = 0.3\mu\text{H}$; $C_1 = 30\text{pF}$; $C_{g1} = 20\text{pF}$

Overhang parameters at rear side: $R_3 = 12.7\text{m}\Omega$; $L_3 = 0.6\mu\text{H}$; $C_3 = 60\text{pF}$; $C_{g3} = 40\text{pF}$

Slot portion parameters: $R_2 = 3.7\text{m}\Omega$; $L_2 = 0.2\mu\text{H}$; $C_2 = 50\text{pF}$; $C_{g2} = 100\text{pF}$ Insulation resistance $R_p = 1\text{G}\Omega$;
Earth Capacitance denoted by C_{gk} , for $k=1,2,3$, etc.

Calculations pertaining to the cable parameters for a cable length of 40m [12]:

i) Series resistance for 1 m of cable is approximately equal to 0.1Ω at a carrier frequency of a few tens of kHz, due to pronounced skin effect. Hence cable resistance can be put at 4Ω .

ii) Self inductance of the cable would be $13.6\mu\text{H}$; since the self inductance of a 3 core cable with 1.5mm^2 conductor would be 0.34mH/km .

iii) Value of capacitance remains unaffected due to frequency. Capacitance of one conductor in relation to others and lead sheath for a 3-core 1.5mm^2 cable is $0.17\mu\text{F/km}$. Hence capacitance of the cable conductor for the model can be taken to be 6800pF .
Cable parameters: Length=40m; $R_{c/ph} = 4\Omega$; $L_{c/ph} = 14\mu\text{H}$; $C_{/ph} = 6800\text{pF}$.

Further, the cable is divided into 10 sections of each 4m and the parameters assigned for each

individual segment. This approach yields better results that are better than considering the whole length of the cable as a lumped parameter. Further a distributed parameter assignment gives results that are closer to experimental results. Effect of mismatch between the cable and the motor surge impedances is also taken into account. Reduction in voltage distortion by the introduction of matching impedance at the cable-motor junction has also been tried out; to see the effect of such a matching in modifying the line end coil voltage waveform. This also helps in studying the effect of the cable in attenuating the input carrier waveform in magnitude and modifying the rise time of the pulse that reaches the motor terminal.

2.2 Modification of line end voltages – Computer Simulation

The source selected is a square pulse generator, to represent the carrier waveform of a pulse-width-modulated inverter. The generator output is fixed at 15V, with a frequency of 15kHz and 50% duty cycle. The rise time and the fall time of the pulse is 60ns. Winding configuration considered is connection in delta, which is common with the induction motors. The line end voltage waveforms are recorded for inter-turn faults created at various points in the winding starting from the line end. The faults are created by reducing the insulation resistance shunting the capacitance of the interturn insulation gradually from a healthy 10^9 ohms to 1000 ohms. The line end voltage waveforms are recorded using the grapher in MULTISIM software. The insulation resistance values selected are $10M\Omega$, $1M\Omega$, $100k\Omega$, $10k\Omega$ and $1k\Omega$. This exercise is repeated by creating faults at various places in the three turns of the line end coil model. The oscillatory stator voltage waveforms in the simulation oscillograms are exported to the spreadsheet environment for further study and analysis.

Simulation results show that the line end coil voltage waveforms between $1G\Omega$ to $1M\Omega$ rarely showed any difference. Further, incorporating all the waveforms pertaining to all the values of the insulation resistance cluttered the oscillograms and cramped the necessary information. Hence, only values of $10M\Omega$, $100k\Omega$ and $1k\Omega$ were selected for display in the oscillograms pertaining to simulation.

2.3 Modification of line end voltages – Motorette and Experimental setup details

The motorette used is a fully wound stator of a 1.5HP, 3-phase motor. The stator has 36 slots. The winding configuration uses 3coils/pole/phase in a 4-pole arrangement. Each coil is wound with 50 turns since it is known that the initial voltage distribution does not see beyond a few turns of the line end coil [11]. The R, Y, B phase windings are of mushroom or basket type. Tappings are taken out of the first three turns of the line end coil of each winding to facilitate measurement. All the junctions of the coils in all phases are also accessible through tappings taken. The motorette is shown in figure 5.

A low voltage square pulse generator with 15V peak output and at 15kHz is used. A 40m long PVC covered wire is used to connect the pulse generator to the motorette. The square pulse has a rise time of 60ns. The oscilloscope used is a 60MHz dual channel digital storage oscilloscope with tuned

1:1 probes and connected to the cable side of the line end coil. The test set-up is shown in figure 6. Input waveform at cable side of the line end coil is shown in fig.7.

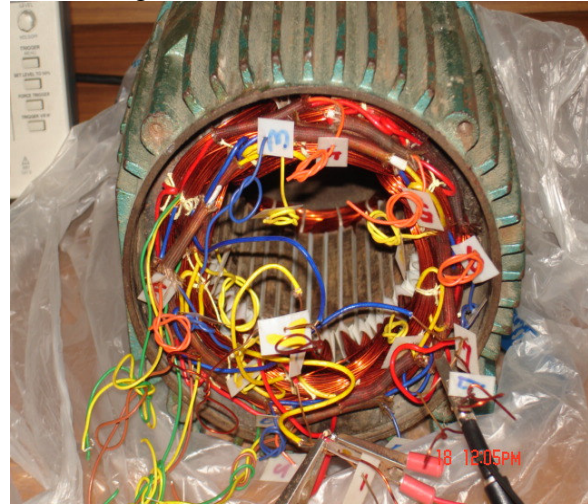


Fig.5 Motorette



Fig.6 Test Set-up

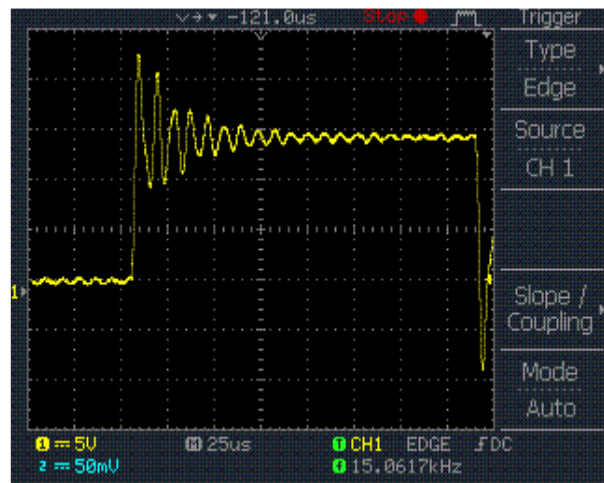


Fig.7 Input Waveform

Fixed resistors of nominal values 10MΩ, 1MΩ, 100kΩ, 10 kΩ and 1kΩ are used across the interturn tappings to simulate the effect of degradation in insulation resistance values. For the above five specific conditions, the line end coil voltage

waveforms are measured in the line end coils of R and B phases. The oscilloscope readings are taken to the spreadsheet environment in the personal computer through manufacturer’s interfacing software.

3. Simulation and Experimental Results

Modification of cable-end voltage waveforms of line end coil due to inter-turn faults

3.1 Oscillograms related to R-phase

Cable end voltage waveforms for fault at junction of 1st and 2nd Turns at R-phase start:

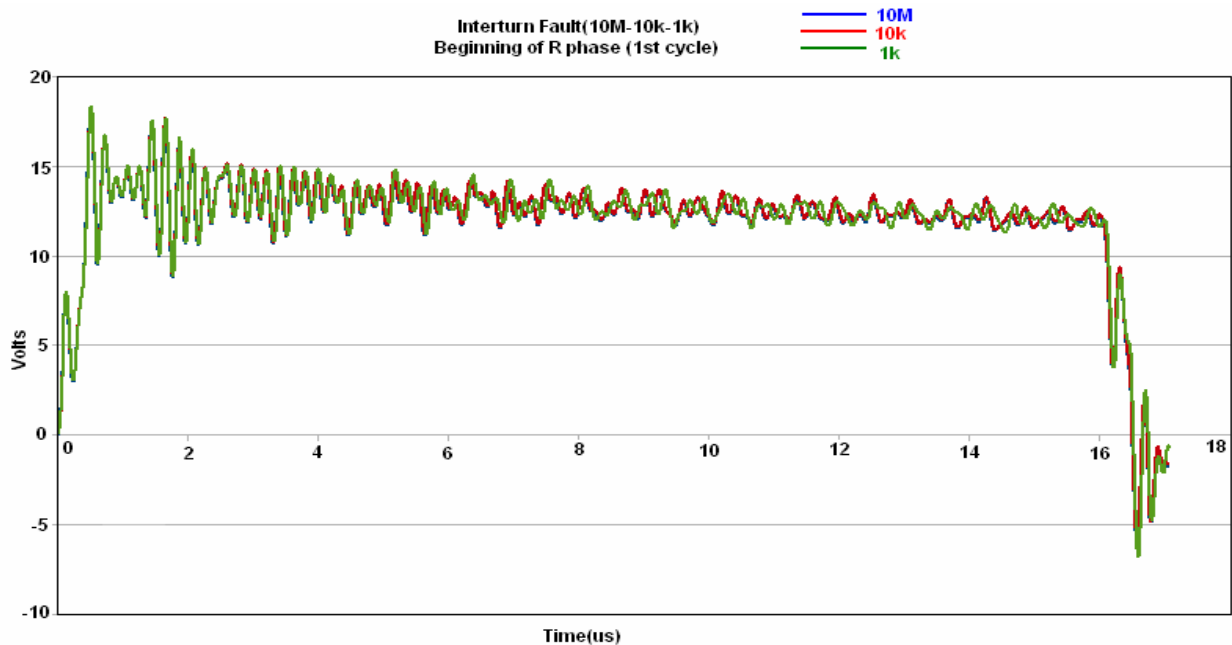


Fig.8 Simulation Results

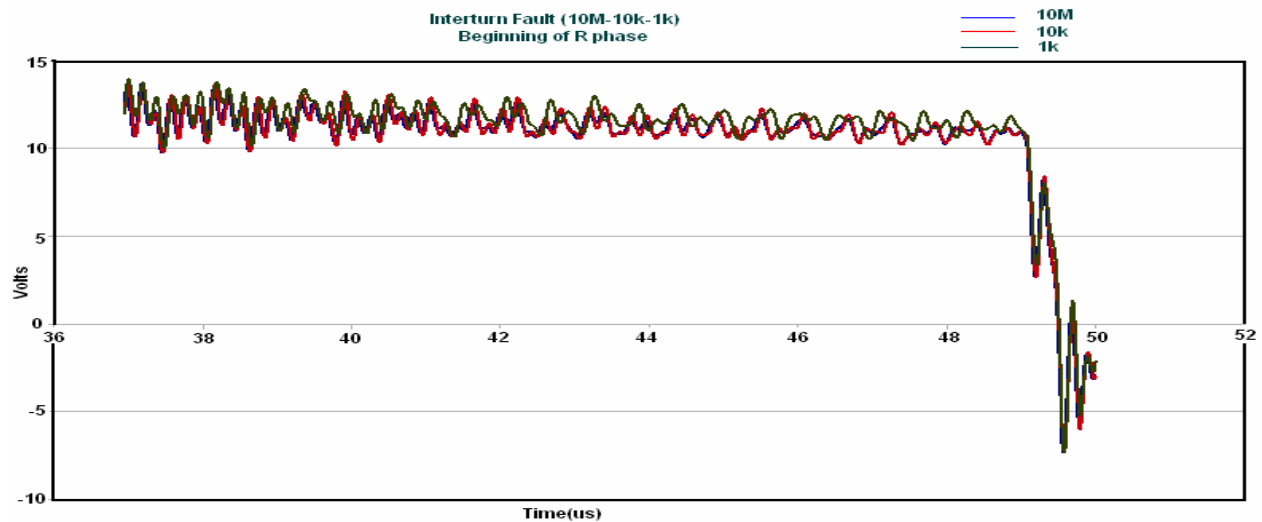


Fig.9 Simulation Results

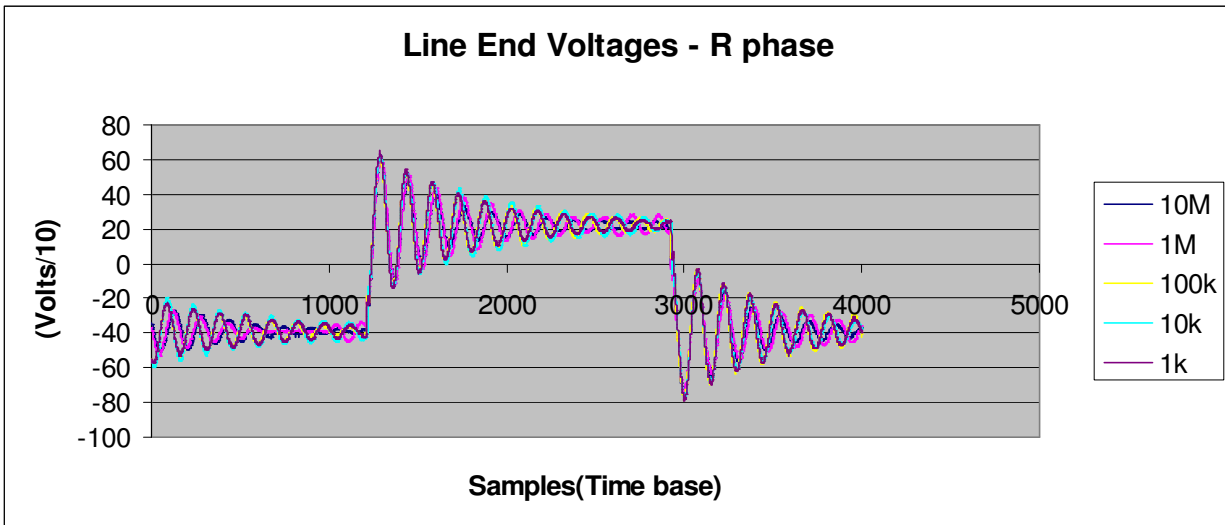


Fig.10 Experimental Results

3.2 Oscillograms related to B-phase

Cable end voltage waveforms for fault at junction of 1st and 2nd turns at B-phase start:

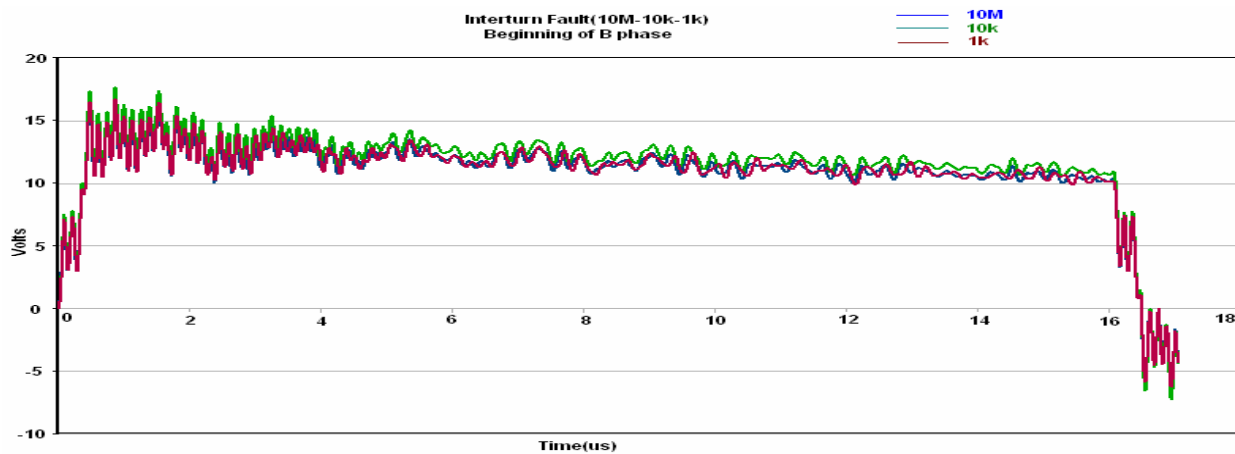


Fig.11 Simulation Results

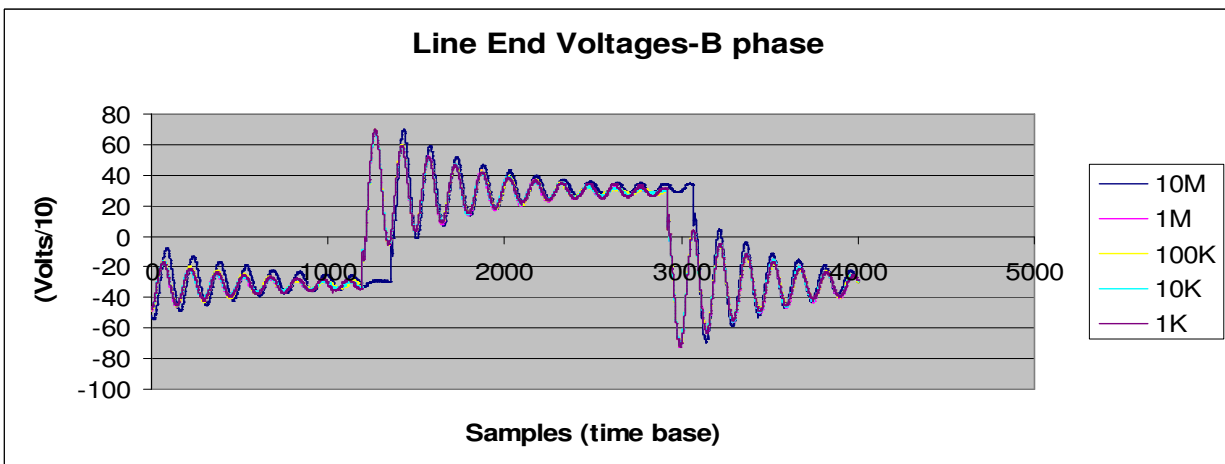


Fig.12 Experimental Results

4 Justifications for the methodology of evaluation used

The IR test measures the resistance of the electrical insulation between the copper conductors and the core of the stator or rotor. Ideally the value of this resistance is infinite since the purpose of the insulation is to block current flow between the copper and the core. But in practice, it is not possible. However, the resistance should have a high value to avoid appreciable leakage current. Lower value of IR indicates that the insulation has deteriorated. A value of $5M\Omega$ is considered as a satisfactory value for the insulation of windings of machines with random-wound coils and form-wound coils rated below 1kV [13].

The interpretation is that while the insulation resistance (IR) is above $1M\Omega$, the interturn insulation is healthy [13]. When the IR value is between $1M\Omega$ and $10k\Omega$, the insulation is good but has started deteriorating. When the IR value is less than $1k\Omega$, the insulation has become weaker and insulation failure is inevitable.

In the model, cable to motor winding impedance mismatching is high ($Z_{cable}=51\Omega$ and $Z_{winding}=108\Omega$). Hence the cable is terminated using its surge impedance value. This is done to get rid of reflections from the motor and cable junction. In service conditions, such a matching may not be resorted to due to additional losses in the terminating impedance. However, the modifications to line end coil voltage waveforms due to reflections makes it easier to identify the effect of reduction in insulation resistance. The approach adopted in this paper of using matching impedance is to reduce the magnitude of extremely high oscillatory voltages caused due to mismatch at cable and motor junction.

Input signal used is a train of square pulses from a signal generator. The rise time of the pulse is 60ns and the nominal frequency is 15kHz. These parameters were chosen to replicate the switching speed of IGBTs (typically 50ns) and carrier frequency used (typically between 10 and 20kHz). The signal wave shape is shown in fig.7.

5 Discussions on results

5.1 R-phase

Oscillograms in fig.8 (time instance between 0 and $17\mu s$) show the effect of interturn fault at the beginning of R-phase. While the difference in the pattern of the waveforms between $10M\Omega$ and $10k\Omega$ is negligible, there is a marked difference between

waveforms pertaining to $10k\Omega$ and $1k\Omega$. Considering oscillograms in fig.9 (36 to $50\mu s$), a small discernable difference has started showing for waveform patterns between $10M\Omega$ and $10k\Omega$. This difference becomes more pronounced in the subsequent cycles due to the effect of reflected waves from other phases.

The pattern in oscillograms pertaining to figs.8 and 9 is confirmed by the experimental result shown in fig.10. While the difference in the initial waveform pattern is marked for low values (typically a few $k\Omega$) of insulation resistance for oscilloscope samples between 1000 and 3000, such a difference has started emerging only towards the latter half of the waveform for higher values of insulation resistance (typically a few $M\Omega$) as seen between DSO samples 3000 to 4000.

A comparison of figs.8, 9 and 10 shows that while the insulation resistance values are healthy (typically above $1M\Omega$), the line end coil voltage waveform pattern is nearly the same. Subsequently, when the degradation in insulation strength starts showing (typically between $1M\Omega$ and a few $k\Omega$), the patterns start showing a difference after a few cycles. When the insulation degradation has progressed to a non-recovery level (typically lower than a few $k\Omega$), the difference in waveform pattern shows up right in the beginning of waveforms due to the high damping of high frequency capacitive current by the low value of insulation resistance; markedly elongating the waveform oscillations towards the end of the cycle.

5.2 B-phase

Considering the interturn fault at the beginning of B-phase, waveforms for this condition is shown in figs. 11 and 12.

With reference to the oscillograms shown in fig.11, all waveforms pertaining to insulation resistance values of $10M\Omega$, $10k\Omega$ and $1k\Omega$ have started showing different patterns in the first cycle of carrier waveform; though the difference between waveforms pertaining to $10k\Omega$ and $1k\Omega$ is more marked. Such behaviour is corroborated by experimental results shown in fig.12.

The behaviour seen in figs.11 and 12 are due to reflected waves from the beginning of B-phase (in about 460ns) to the line end coil in R-phase (about 168m of winding length and the stator core essentially acting like an air core for high frequencies). These reflected waves void of high

frequency content, modify the line end voltage waveform.

5.3 Comments related to actual service conditions

Under actual service conditions, the carrier waveforms (essentially square pulses either through filters or without filters) will form the sinusoidal envelop. Hence, while two phase voltages might be positive, one will be negative. Such a condition would either produce a situation similar to the 1- Φ modeling shown in simulation or show up marked difference in waveform pattern due to the negative voltage. Further, long cables will have a certain level of mismatch with the motors and produce additional oscillations. Such a condition would make the difference in line end coil voltage waveform pattern more pronounced.

In practice, the interturn insulation will contain both a capacitance value and a resistance value. Nearly all good insulating materials fail by ageing due to tracking which ultimately lowers the interturn leakage resistance. Such a lowering of the insulation resistance does not affect the capacitance value since the capacitance is due to the geometry of electrodes (bare wire) and insulation. Hence the exercise of only modifying the insulation resistance as done in the paper stands justified. Further, the Insulation Resistance (IR) test uses a dc source which all the more relies on changes in the leakage current. Most of the insulation failures start with an increase in leakage current unless there are defects in the enameled wire insulation either due to bad raw material or poor workmanship.

6 Conclusions

- Adjustable Speed Drives (ASDs) induce transient over voltages that penetrate into the motor winding through oscillatory and traveling wave modes.
- Interturn faults in such random wound motors can develop into earth faults in the coil crossing sections of overhang region.
- There is always a finite level of mismatch between cable and motor surge impedance that can aggravate the stress due to surges.
- An elaborate model of line end coil allows for a better study of the effect of insulation degradation on line end coil voltage waveforms.
- The waveforms obtained through simulation and those generated by experiments agree in their pattern to a great extent, thus validating the models used in simulation.
- Predictions made on the insulation degradation using simulation waveforms will have the ability to forecast a possible impending insulation failure; by comparing between the online measured waveforms.
- Line end coil voltage waveforms show little difference in their pattern when the interturn insulation is healthy.
- Line end coil voltage waveforms show a marked difference in their pattern, when the insulation resistance starts reaching unsafe values.
- Use of line end coil voltage waveforms to monitor interturn faults is a very simple and straightforward method compared to the use of monitoring stator current. The stator current method is either very involved or has limitations to be used as an online method.
- The study of patterns in the line end coil voltage waveforms is amenable for use as an online monitoring method. Waveforms obtained can always be analyzed in an online manner using signal processing method coupled with soft computing techniques. (This work is currently under progress in author's laboratory).

References:

- J. Weed, *Prevention of Transient Voltages in Windings*, Trans. AIEE, vol. 41, 1922, pp. 149-159.
- Melfi, M., Sung, J., Bell, S., Skibinski, G., *Effect of Surge Voltage Rise Time on the Insulation of Low Voltage Machines Fed by PWM Converters*, IEEE Industrial Applications Meeting, Vol.1, 1997, pp.239-246.
- Sidney Bell, Jason Sung, *Will Your Motor Insulation Survive a New Adjustable-Frequency Drive?*, IEEE Trans. Industrial Applications, Vol.33, No.5, 1997, pp.1307-1311.
- Lowery, T.F., Petro D.W., *Application Considerations for PWM Inverter-Fed Low Voltage Induction Motors*, IEEE Trans. Industrial Applications, Vol.30, No.2, 1994, pp.286-293.
- Thorsen, O. V., Dalva, M., *A survey of faults on induction motors in offshore oil industry, petrochemical industry, gas terminal and oil refineries*, IEEE Trans. Industrial Applications, Vol. 31, No. 5, 1995, pp. 1274-1279.

- [6] Stone,G.C., *Recent Important Changes in IEEE Motor and Generator Winding Insulation Diagnostic Testing Standards*, IEEE Trans. Industrial Applications, Vol.41, No.1, 2005, pp. 91-100.
- [7] Randy R. Schoen, et al., *An unsupervised on-line system for induction motor fault detection using stator current monitoring*, IEEE Trans. Industrial Applications, Vol.36, No.6, 1995, pp.1280-1286.
- [8] Ondel, O., Boutleux, E., Clerc, G., *A method to detect broken bars in induction machine using pattern recognition techniques*, IEEE Trans. Industrial Applications, Vol.42, No.4, 2006, pp. 916-923.
- [9] IEEE Std. 522-2004, *Guide for Testing Turn-to-Turn Insulation on Form Wound Stator Coils for Alternating Current Rotating Electrical Machines*, 2004.
- [10]Oyegoke.B.S., *A Comparative Analysis of Methods for calculating the Transient Voltage distribution within the Stator Winding of an Electric Machine subjected to Steep-Fronted Surges*, Proceedings of the 8th International Conference on Electric Machines and Drives, 1-3 September, Cambridge, U.K. IEE Publication No. 444, 1997, pp.294-298.
- [11]Ponnuswamy Rajkumar S., Ebenezer Jeyakumar A., *Stress due to transient voltage distribution in the windings of random wound motors fed by PWM Converters*, International Journal of Electrical and Power Engineering © Medwell Journals, 2(5), 2008, pp.327-332.
- [12]*Chapter 8.7 on Power Cables*, Siemens Electrical Engineering Handbook, Wiley Eastern Limited. Fifth Reprint, 1993, pp.467-476.
- [13]IEEE Std. 43-2000. *IEEE Recommended Practice for Testing Insulation Resistance of Rotating Machinery*, 2000, Table 3.

Acknowledgement

The authors wish to thank the Management for having been a source of inspiration and help, in bringing out this paper.